Turboexpander for Direct Cooling in Hydrogen Vehicle Fueling Infrastructure

Matthew Post,[1] Daniel Leighton,[1] Gabriela Bran-Anleu,[2]
Ethan S. Hecht,[2] Steven Wiryadinata,[2] Brian D. Ehrhart,[2]
and Tom Conboy[3]

1 National Renewable Energy Laboratory
2 Sandia National Laboratories
3 Creare LLC

Turboexpander for Direct Cooling in Hydrogen Vehicle Fueling Infrastructure

Matthew Post,[1] Daniel Leighton,[1] Gabriela Bran-Anleu,[2] Ethan S. Hecht,[2] Steven Wiryadinata,[2] Brian D. Ehrhart,[2] and Tom Conboy[3]

1 National Renewable Energy Laboratory
2 Sandia National Laboratories
3 Creare LLC

1.   INTRODUCTION

Hydrogen fuel cell electric vehicles (FCEVs) have been identified as one of a few options for zero carbon emissions transportation. A major advantage of FCEVs is that they can fuel quickly and follow a familiar fueling behavior to hydrocarbon-fueled vehicles. Whether light duty or heavy duty, the goal for a hydrogen dispenser is to fuel a vehicle in the same amount of time as the fossil fuel equivalent. When hydrogen is dispensed into the vehicle storage system, however, the temperature rises due to the Joule-Thomson effect and the heat of compression. Typically, vehicles store the compressed hydrogen in composite overwrapped pressure vessels that have a polymer liner with an operational temperature limit of 85°C [1]. This temperature limit can be exceeded during fast fueling if hydrogen is not precooled. Precooling allows for a dispenser to fuel a vehicle at a faster flow rate by preventing the storage tank on the vehicle from overheating. Fueling protocols and requirements are presented in SAE J2601 Fueling Protocols for Light Duty Gaseous Hydrogen Surface Vehicles [2]. A heavy-duty equivalent is under development with similar requirements for precooling [3]. Currently, conventional precooling for light-duty vehicle refueling uses a heat exchanger and chiller to cool the hydrogen gas to -40°C before entering the vehicle. The precooling system represents a significant part of the station capital and operating costs, so if the cost of the precooling system can be reduced by improving its efficiency, the overall station capital and operating cost can be reduced.

In this project, National Renewable Energy Laboratory (NREL) and Sandia National Laboratories (SNL) researchers teamed up to investigate the turboexpander precooling application. A turboexpander is a device that places a turbine in a flow path where a pressure differential can be attained. This expansion device will extract work and lower the temperature of the fluid as the pressure reduces. While initial calculations based on established principles showed potential for a turboexpander to generate cooled gas, much work needs to be done to prove the concept. Turboexpanders typically work best under steady state conditions, while the dispenser is a very dynamic flow system. Dynamic turboexpander systems have been proven, such as a turbocharger on a gasoline vehicle. The inlet pressure at a dispenser is also much higher than any other known turboexpander system but should behave similarly to higher density fluids at lower pressures.

Having both performed initial calculations, NREL and SNL researchers teamed up to investigate the turboexpander precooling application further. A project was soon built around the idea with SNL performing system modeling using previously proven capabilities and NREL performing hardware characterization with established station capabilities. Creare LLC was contracted as the turbomachinery expert to design and build the concept device. Part way through the project, however, contracting issues with the funding partner caused the project to terminate early before building and characterizing the concept device. While the project could not continue, many key findings were already learned. This paper is a summary of those findings.

1

2.   SYSTEM MODELING

2.1.   Introduction

A collaborative project between Sandia National Laboratories, NREL, and Creare, LLC, studied the use of a turboexpander precooling system to be used at a hydrogen fueling station to improve efficiency, lower cost, reduce footprint, and improve operation. At Sandia, there were two primary objectives:
- Perform station systems modeling and analysis to identify strategies for integrating the extracted work from the turboexpander during transient operation.
- Determine dynamic temperature fueling strategies made possible by the turboexpander that prevent vehicle tank overheating.

2.1.1.   Integration Strategies

One important metric for justifying the use of a turboexpander in a hydrogen fueling system is the system performance relative to the current station technology. This requires a model for the mass and energy flow of hydrogen into and out of the turboexpander as well as utilities required by the turboexpander. An analogous model for an active chiller is also needed for comparison purposes with a conventional station, as well as additional cooling that might be needed for a station that incorporates a turboexpander. The differences in temperature and pressure of the hydrogen on either side of the cooling hardware are the critical metrics for each of these cooling options. The heat rejection and extracted work from the turboexpander are also important performance metrics of the turboexpander. The pressure drop (and pressure leakage), the efficiency of the extracted work, and the thermal losses are important characteristics of the system. These characteristics are unknown for a real system, so the values can be varied in modeling studies in order to ascertain the desired performance envelope and trade-offs within the system. Comparisons of the turboexpander system to current state-of-the-art active chillers can highlight improvements to the efficiency of the refrigeration cycle and reductions in the utility electricity required. This modeling allows for a direct comparison of a turboexpander to a conventional system at identical conditions.

2.1.2.   Fueling and Operation Strategies

During conventional fueling, hydrogen that flows into the vehicle tank is cooled at the station to a constant low temperature (ideally around -40°C), so that tank walls do not overheat when the hydrogen gas expands into the vehicle tank. Heating can degrade the safety and performance of the liner material for the on-board vehicle tank. With a turboexpander, the temperature of the hydrogen flowing into the tank could be more dynamic than a conventional cooling system, and so modeling is needed to ensure tank safety when using this technology. MassTran, a Sandia-developed Python code [4], was used to model tank filling to further inform the turboexpander design efforts. MassTran is able to model compressible flows in networks consisting of pressure vessels, connecting tubing, orifices, valves, and flow branches. The model was used to predict the pressure and temperature of the hydrogen in the tank, as well as the tank wall temperature as a function of time. MassTran results show whether the outlet pressure and temperature of the turboexpander system are sufficient to fully fill the vehicle tank (maximum pressure of 70 MPa) in 5 minutes while maintaining tank temperatures below the limit of 85°C.

2

2.2. Model Description

2.2.1. Integration Strategies

A Python-based model was developed to assess the energetic and exergetic performance of the baseline and alternate systems for a single set of inputs. The model performs a steady-state thermodynamic analysis of the hydrogen (H_2) and refrigerant (R32, assumed) streams across a defined control volume and at specific state points (Figure 1). H_2 flows into the system at boundary 2 and is compressed to the design pressure in cascade storage cylinders. The electrically driven compressor is modeled as a pseudo-single stage compressor with a user-specified efficiency and degree of intercooling. Subsequent analysis of the input stream is split according to user-specified mass flow fractions. In the baseline case with only a conventional chiller (Figure 1, top), the pressure is reduced to the dispenser pressure for each of the three cascade groups via isenthalpic valves. In the alternate case (that includes the turboexpander - Figure 1, bottom), the pressure reduction is achieved via the turboexpander (the diagram shows the turboexpander model for each cascade pressure level) connected to an electric generator for work recovery. In the initial analysis, a chiller system provides additional cooling to the H_2 stream via a heat exchanger after the turboexpander in order to maintain a -40°C flow at the dispenser. The model considers user-specified pressure drops and heat losses between relevant state points.
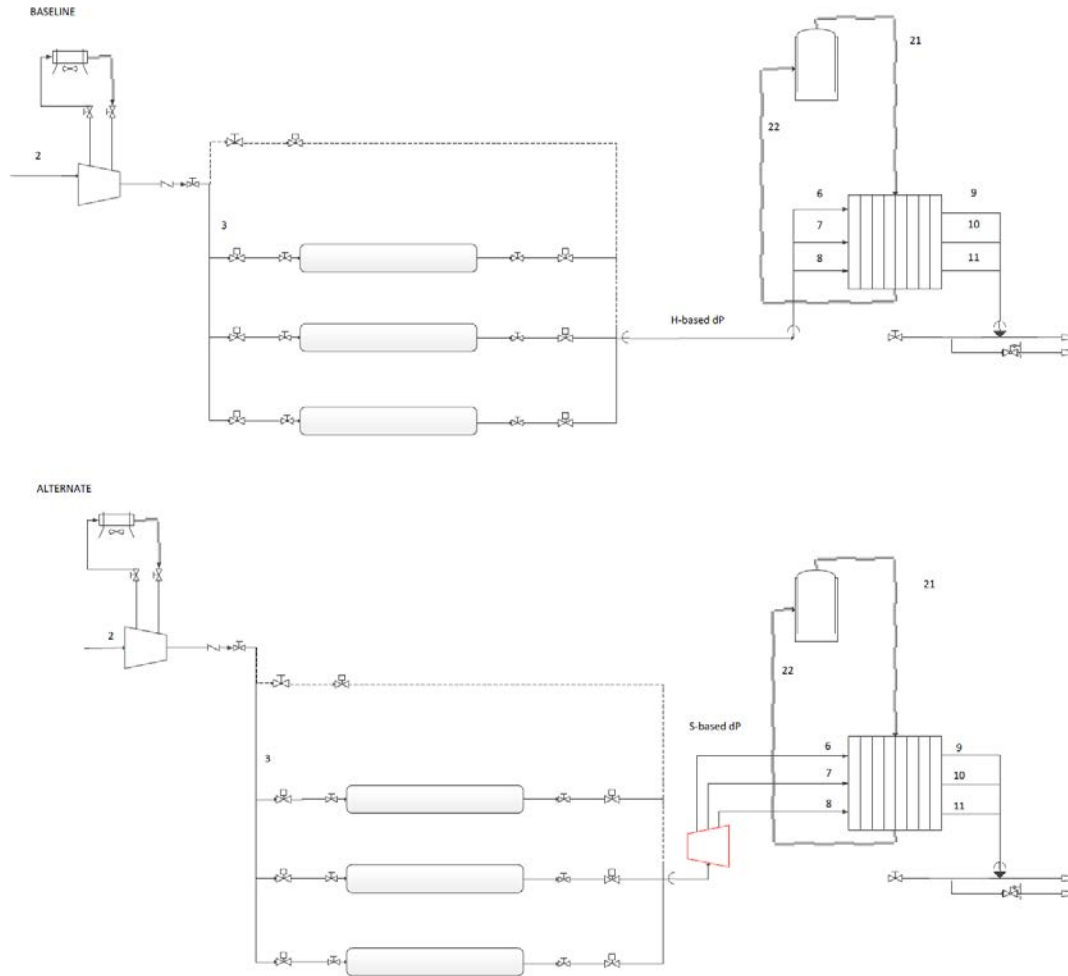
3

Figure 1. Control volume of analysis and state points for the conventional system (top) and turboexpander system (bottom).

The capacities of the compressor and turboexpander as well as the H_2 temperatures at the dispenser are calculated based on user-specified operating conditions in order to facilitate coupling to the tank filling model described in the next section. User specification of the compressor, turboexpander, and chiller capacities are also possible to calculate the flow conditions (i.e., temperature response) of H_2. The overall plant exergy efficiency is calculated as the change in H_2 specific exergy across the system boundary over the net electrical input power by the compressor, turboexpander, and chiller.

2.2.2. Fueling and Operation Strategies

MassTran is a third-generation piping network flow modeling tool that has been developed at Sandia National Laboratories [4]. MassTran can model compressible flows in networks consisting of pressure vessels, connecting tubing, orifices, valves, and flow branches. MassTran was developed to replace a Fortran code called NetFlow [5], and while a tank filling model for NetFlow was validated, MassTran was unvalidated for this application. Further, when NetFlow was converted to Python, the wall heat conduction model was not a priority, so it was not included in the MassTran package. As this wall heat conduction model was critical for the needs

4

of this project, this modeling capability was added into the python MassTran framework, as described below.

2.2.2.1. Wall Heat Transfer

MassTran assumed a constant wall temperature and no heat transfer to the environment. In order to explore tank filling under different environmental conditions, the 1D transient heat conduction model described in Reference [5] was added to the MassTran code. It is assumed that heat conduction flows along a line normal to the interior wall as shown in Figure 2. The wall can be constructed of several layers with different material properties and different thickness. For a hydrogen tank, the wall was divided into two layers, the liner and carbon fiber reinforced polymer (CFRP).
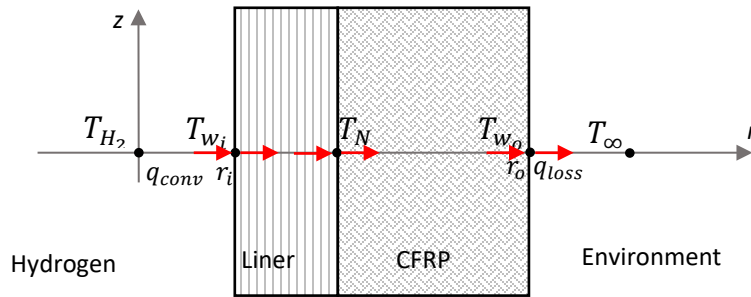

Figure 2. Heat transfer model used to calculate the temperature profile across the wall of a hydrogen tank.

The governing transient energy equation is used to solve for the wall temperature profile T_w,

$$\rho_w c_{p,w} \frac{\partial T_w}{\partial t} = -\frac{1}{r^2} \frac{\partial}{\partial r}\left(k_w r^2 \frac{\partial T_w}{\partial r}\right) \tag{1}$$

where ρ_w, $c_{p,w}$, and k_w are the density, specific heat, and thermal conductivity of the wall material, respectively. At time $t = 0$ seconds, the wall temperature is assumed to be equal to the gas temperature. The following heat convection equations are used as boundary conditions for equation (1)

$$q_{(r=r_i)} = A_{c,r_i} h_g\left(T_{H_2} - T_{w_i}\right) \tag{2}$$
$$q_{(r=r_o)} = A_{c,r_o} h_\infty\left(T_{w_o} - T_\infty\right) \tag{3}$$

where h_g is the heat transfer coefficient between the gas and the interior tank wall surface area, A_{c,r_i}, and h_∞ is the heat transfer coefficient at the exterior tank wall surface area, A_{c,r_o}. T_{H_2}, T_{w_i}, T_{w_o} and T_∞ are the temperatures of the hydrogen gas, the inner wall, the outer wall, and the environment where the vehicle tank is located, respectively.

The thermal properties of the wall, the temperature of the outside environment, and the heat transfer coefficient for the outer tank wall to the environment are assumed to be constant.

5

The heat transfer coefficient for the interior tank wall surface was calculated using the following Nusselt correlation [6],

$$\text{Nu}_{D_{int}} = \frac{h_g D_{in}}{k_g} = 0.17\text{Re}_{d_{in}}^{0.67} \text{ for } 2.6 \times 10^4 < \text{Re}_{d_{in}} < 7.1 \times 10^5 \tag{4}$$

where D_{in} is the inner pressure vessel diameter, k_g is the thermal conductivity of the gas. The Reynolds number is based on the injection diameter, d_{in}, and is defined as,

$$\text{Re}_{d_{in}} = \frac{\rho_g v d_{in}}{\mu_g} = \frac{4\dot{m}}{\pi \mu d_{in}} \tag{5}$$

The gas density, ρ_g, and gas viscosity, μ_g, are calculated at the bulk temperature and pressure inside of the pressure vessel.

2.2.2.2. Validation

The MassTran model was validated using the experimental results obtained by Johnson et al. [7] which was a rapid filling of high-pressure hydrogen tank experiment. MassTran was used to simulate the fast filling of a 36.9 L type IV tank, with a 3.8 mm-thick plastic liner, and a 23.5 mm-thick wrapping of carbon-fiber reinforced epoxy composite (CFRP). The length and inner diameter of the tank are 905 mm and 319 mm, respectively. A 1.3 mm-orifice tank-size was used [2]. The thermal properties of CFRP and the plastic liner are specified in Table 1.

Table 1. Material Properties of CFRP and plastic liner [2].

	CFRP	Plastic Liner
Density (kg/m³)	1256	941
Thermal Conductivity (W/m-K)	0.69	0.48
Specific Heat (J/kg-K)	1578	2000

The initial pressure and temperature inside the tank are assumed to be 4.99 MPa and 27.9°C, and that the hydrogen inlet temperature is 20.3°C.

Figure 3 compares the numerical results with the experimental results obtained by Johnson et al. [7]. As shown in Figure 5 (left), the gas temperature is well predicted at early times, although there is some deviation at later times. This effect can likely be corrected by accounting for the heat loss from the tube that connects to the tank orifice. The wall temperature is also well predicted by MassTran as shown in Figure 5 (right). There is some variation in the experimental measurements that could be partially attributed to noise but is more likely due to the highly turbulent mixing within the tank during the filling process. The model dampens out any of the fluctuations, reporting only a mass averaged temperature.
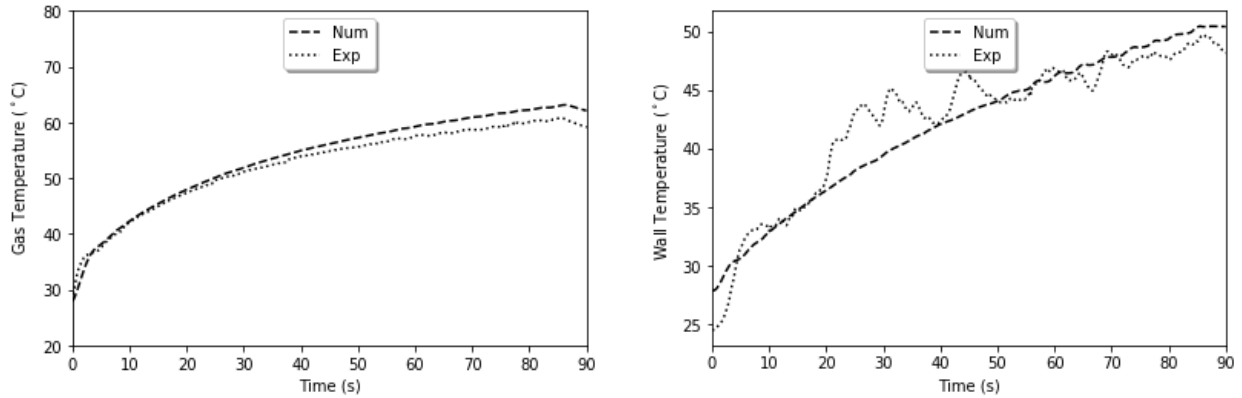
Figure 3. Comparison between experimental and numerical results of the gas temperature (left) and wall temperature (right) as a function of time.

The Hydrogen Station Equipment Performance (HyStEP) device has been used to certify hydrogen dispensers. This device contains tanks that are used for this certification process, and data from these tanks was used to further validate the MassTran tank model. Two temperatures were measured at two different locations inside of the hydrogen tank during filling. The mass-averaged temperature obtained with MassTran was compared to the measured temperatures at specific locations in the tank. The numerical results were compared to three data sets. The first data set was obtained from a filling where the initial tank temperature was -7°C. The second data set was obtained from a filling where the initial tank temperature was 27°C to ensure that at higher initial temperatures, MassTran can still be able to predict the temperature rise, and that the temperature is still below the requirements. Figure 4 shows the experimental data compared to MassTran predictions for these two data sets. A third data set used was a filling of a two-tank bundle and is shown in Figure 5. As shown in these figures, MassTran can predict tank temperatures fairly accurately within the experimental variability.
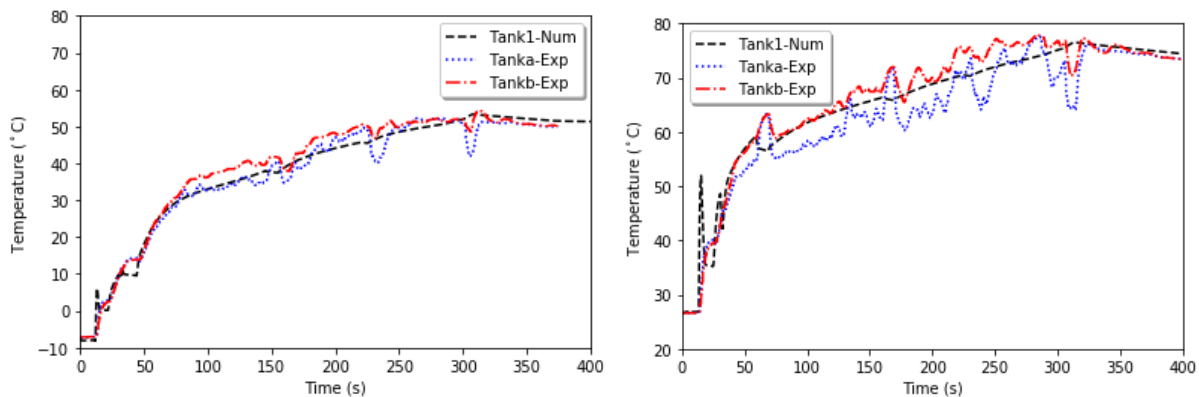

Figure 4. Tank temperature as a function of time for the filling of a tank initially at -7°C (left) and a tank initially at 27°C (right).
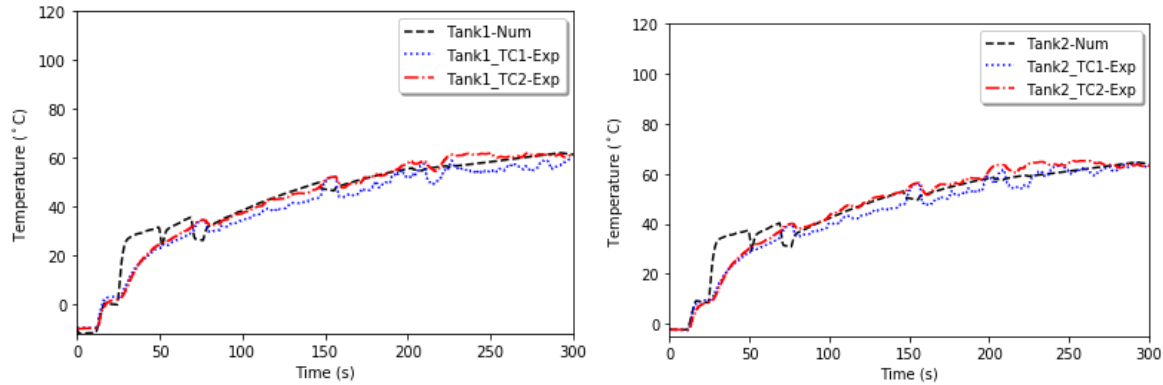
7

Figure 5. Temperature inside tank 1 (left) and tank 2 (right) as a function of time during the filling of a two-tank buddle.

2.3. System Modeling Results

The model described in section 2.1.1 was used to perform a thermodynamic analysis of the hydrogen (H_2) and low-temperature refrigerant streams (used to precool the hydrogen) during tank refueling.

Referring to Figure 1, H_2 flows into the system at boundary 2 and is compressed to the design pressure in cascade storage cylinders while the refrigerant is circulating through points 21 and 22. In the baseline case with only a conventional chiller, the pressure is reduced to the dispenser pressure for each of the three cascade groups via isenthalpic valves. In the alternate case (that includes the turboexpander), the pressure reduction is achieved via the turboexpander expansion while work recovery is achieved via an electrical generator. Transient analysis was performed with a series of steady-state analyses at varying dispenser pressures. For each dispenser pressure, the model includes a calculation of the overall plant exergy efficiency (defined as the change in H_2 specific exergy across the system boundary over the net electrical input power by the compressor, turboexpander, and chiller).

Preliminary system operation parameters for the thermodynamic model were selected based on the H2FIRST reference station design [8] and are shown in Table 2. The preliminary energy and exergy flows of the existing and alternate systems are presented in Figure 6 and Figure 7, respectively. In order the capture an average exergy flow for the three cascade pressure levels, Figure 8 and Figure 9 represent an average point in the dispenser operation where 2 of the 4 dispenser hoses are supplying at the low pressure cascade tank limit (33 MPa), one at the medium pressure limit (61.3 MPa), and the remaining at the high pressure limit (80.2 MPa - representing simultaneous filling of 4 vehicles at 3 discrete points in time in the filling sequence).

Table 2. System specifications for baseline and alternate cases.

	baseline	alternate	units
Ambient			
Pressure	0	0	MPa_g
Temperature	15	15	°C
hydrogen			
Initial Pressure	6.89	6.89	MPa_g
Temperature	0	0	°C
Mass flow rate	40	40	kg/hr
operating pressure and initial flow for 3 cascade tanks			
$P_{0, low}$	5.3	5.3	MPa_g

8

|	baseline	alternate	units
$P_{max, low}$	33	33	MPa_g
Y_{low}	1	1	
$P_{0, med}$	33	33	MPa_g
$P_{max, med}$	61.3	61.3	MPa_g
Y_{high}	0	0	
$P_{0, high}$	61.3	61.3	MPa_g
$P_{max, high}$	80.2	80.2	MPa_g
Y_{high}	0	0	
equipment specifications			
compressor			
Isentropic Efficiency	0.75	0.75	
Isothermal Efficiency	0.75	0.75	
Mechanical Efficiency	0.95	0.95	
Motor Efficiency	0.91	0.91	
Condenser Coefficient of Performance	20	20	
Degree of Intercooling	0.9	0.9	
Compression Ratio	13.7	13.7	
Capacity Specified	False	False	
Compressor Capacity	N/A	N/A	kW
cascade			
$DP_{cascade\ low-HX}$	0.6	0.6	MPa
$DP_{cascade\ med-HX}$	0.8	0.8	MPa
$DP_{cascade\ low-HX}$	1	1	MPa
heat exchanger			
$DP_{HX, low}$	0.6	0.6	MPa
$DP_{HX, med}$	0.8	0.8	MPa
$DP_{HX, high}$	1	1	MPa
heat loss to atmosphere (low)	1	1	kW
heat loss to atmosphere (medium)	1	1	kW
heat loss to atmosphere (high)	1	1	kW
dispenser			
$DP_{dispensing\ line}$	0.2	0.2	
chiller			
Refrigerant Type	R507A	R507A	
Capacity	0	0	kW
Setpoint	-40	-40	°C
Evaporator Approach Temperature	3	3	°C
Condenser Approach Temperature	10	10	°C
Isentropic Efficiency	0.75	0.75	
Isothermal Efficiency	0.75	0.75	
Mechanical Efficiency	0.95	0.95	
Motor Efficiency	0.91	0.91	
Coefficient of Performance	20	20	
Degree of Intercooling	0.3	0.3	
Compression Ratio	50	50	
Condenser Coefficient of Performance	20	20	
$DP_{condenser}$	1	1	
subcool temperature	10	10	°C
$DP_{thermal\ expansion\ valve}$	1	1	
turboexpander			
Isentropic Efficiency	N/A	0.85	
Mechanical Efficiency	N/A	0.95	
Motor Efficiency	N/A	0.91	
Specify capacity	N/A	False	
Turboexpander capacity	N/A	N/A	kW
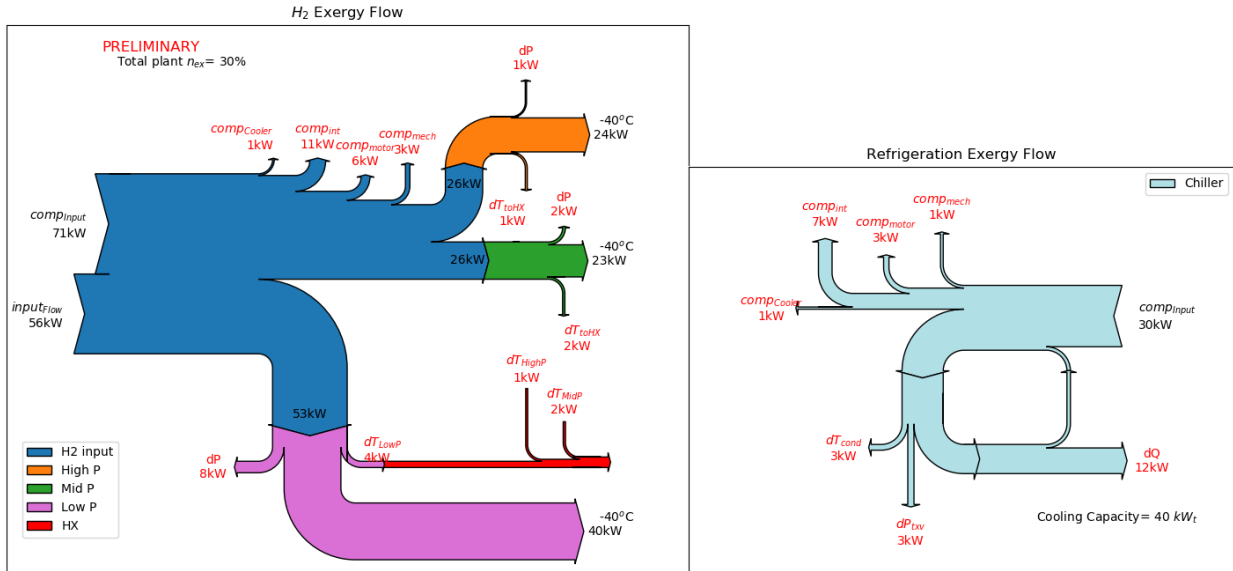
Figure 6. Baseline system H2 exergy flow. Red parameters denote exergy losses through the system.
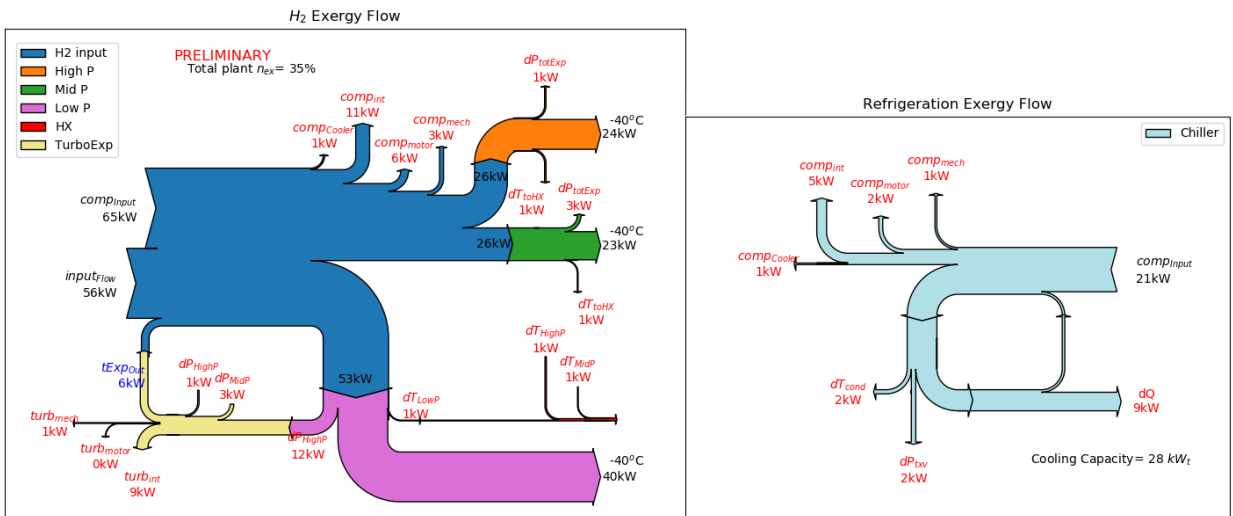

Figure 7. Alternate system H₂ exergy flow. Red parameters denote exergy losses through the system.

This preliminary analysis showed that the conventional fueling station with a chiller is estimated to have an exergy efficiency of 30%. The use of the turboexpander in the alternate case improves this value to 37% due to reduction in chiller load needed to supply -40°C H₂ and recovery of electrical work to offset the upstream compression.

The time progression of temperature, pressure, fueling station power, and overall exergy efficiency are presented in Figure 8 and Figure 9. These figures reflect identical, user-specified pressure ramps (5–70 MPa) and equipment efficiencies (shown in Table 2), with particular changes discussed as follows. Figure 10 is the comparison of the baseline and alternate cases with a cascade (expansion inlet) temperature and pressure of 40°C and 95 MPa, respectively, and no chiller cooling for the alternate case. Due to work recovery of the turboexpander, the alternate

case shows higher efficiency and lower net input power of the fueling system. However, without a chiller providing additional cooling or any thermal buffering, this system does not maintain a delivery temperature of -40°C throughout the filling cycle.

In order to illustrate the influence of station design, an exaggerated over-temperature case was analyzed with the expander input (cascade storage) temperature increased to 135°C (by specifying a lower compressor intercooling), but with a 35-kW$_t$ chiller enabled. In this case, the duration over which the expander can provide gas at <-40°C is significantly reduced. Beyond this, the chiller is increasingly loaded in order to maintain a delivery temperature -40°C. The overall lower exergy efficiency and higher fueling station net power (relative to Figure 8-right) are due to the combination of chiller power draw and increased compressor power draw. Nonetheless, the exergy efficiency of the over-temperature case still exceeds that of the conventional station without the temperature burden (Figure 8-left) until the dispenser pressure exceeds 43 MPa.
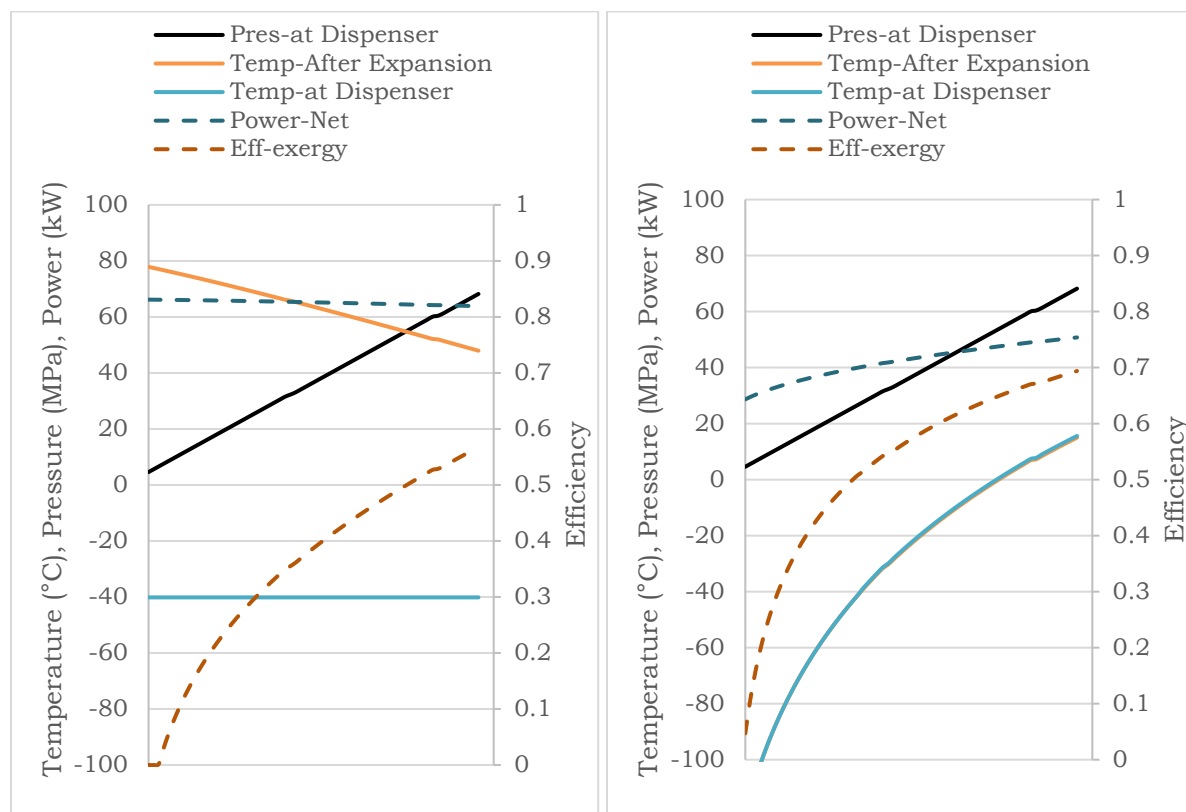

Figure 8. Temperature, power and exergy efficiency of the baseline system (left) and alternate system with no chiller cooling (right). Pressure ramp is identical and cascade temperature is 40°C in both cases. Note: x-axis denotes an arbitrary time step with the assumption of a static system.
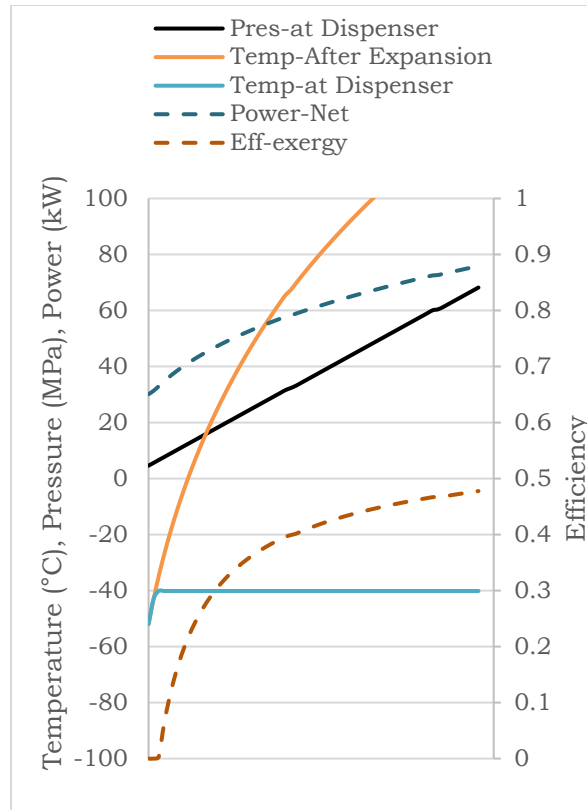
11

Figure 9. Temperature, power and exergy efficiency of the alternate system with a hotter cascade (turboexpander inlet) temperature of 135°C and chiller maintaining -40°C. Pressure ramp is identical to Figure 10. Note: x-axis denotes an arbitrary time step and Temp-After Expansion is deliberately cut off to maintain common ordinate axis range with Figure 10.

The turboexpander should be able to cool down the hydrogen flow to the inlet tank maintain the tank wall temperature below 85°C during filling. Transient temperatures from the dispensing system, such as those shown in Figure 8 and Figure 9, were calculated for turboexpander efficiencies ranging from 40% to 70%, for a modestly cooled 0°C turboexpander inlet temperature hydrogen. The dispenser conditions were then used in the MassTran model to determine the tank temperature rise during the tank filling process. Figure 10 (left) shows the inlet tank temperature as a function of time calculated with the exergy model. For a turboexpander with an efficiency of 40%, the minimum temperature the turboexpander can achieve is -40°C. As time increases, the hydrogen temperature coming from the turboexpander increases (due to a smaller pressure drop) until it reaches a maximum temperature of -10°C at the end of the filling. On the other hand, a turboexpander with a 70% efficiency is able to cool the hydrogen to -105°C at the beginning of the fill. During the filling, the hydrogen temperature coming from the turboexpander increases until it reaches a maximum temperature of -20°C. Figure 10 (right) shows the tank wall temperature as a function of time for different turboexpander efficiencies. Without a turboexpander, the tank inlet temperature would be a steady 0°C, and the tank wall temperature would follow the purple line, rising above 85°C around 175 seconds into the fill. By contrast, a turboexpander with an efficiency of only 40% is able to provide sufficient additional cooling that the tank wall temperature will remain below 85°C. Steady inlet-temperature cases of -40°C and -33°C (i.e., a T40 SAE-J2601 fill) are also

12

shown on the plot, and the combination of a modest, 0°C chiller and additional cooling provided by a 60% efficient turboexpander, results in a similar final tank wall temperature around 60°C. The turboexpander improves the efficiency at the station and reduces the cooling requirements to be provided by a conventional chiller and heat exchanger.
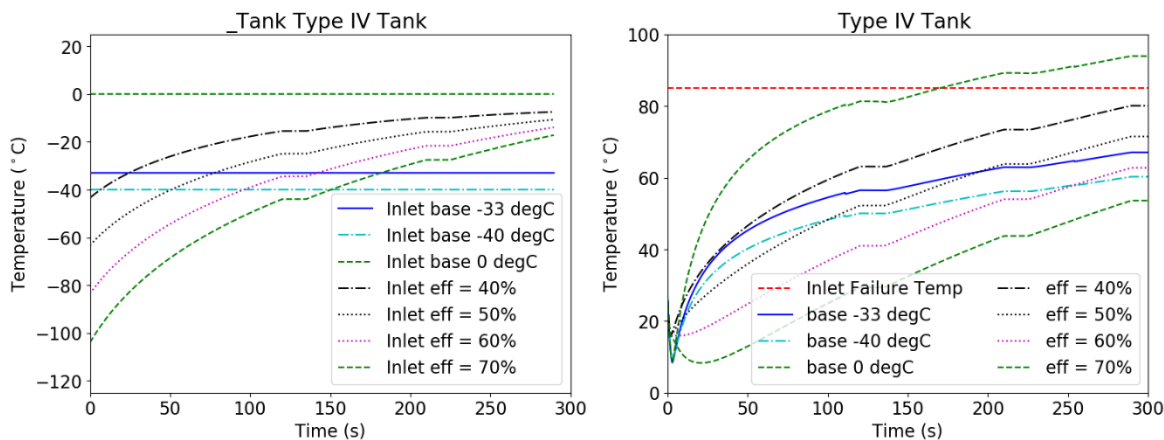

Figure 10. Left: Inlet tank temperature as a function of time obtained using the Exergy Model for turboexpander efficiency ranging from 40% to 70%, along with two base-cases with a steady hydrogen inflow temperature of 0 and -40 deg C. Right: MassTran calculated tank wall temperatures using inlet temperatures from Exergy Model (left).
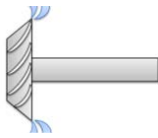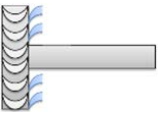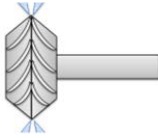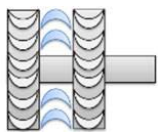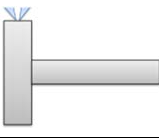
2.4.   Modeling Conclusions

The operational parameters used in this work (i.e., those shown in Table 2) are expected to be appropriate for hydrogen dispensing systems, but the models should be exercised for sensitivities to these parameters, and as experimental data is gathered, updated. The efficiency of the turboexpander was varied from 40-70% in this work, but real-world designs and testing of a turboexpander in this application is needed to measure achievable efficiencies. As the MassTran modeling showed in this work, unsteady temperature flows to a tank can result in safe fills with tank wall temperatures being maintained below 85°C. Therefore, fueling protocols must be developed that can take advantage of the transient temperature flows that can be achieved with this turboexpander technology. There may be challenges developing turbomachinery designed for the low flowrates of light-duty fuel cell electric vehicle tanks. It is likely that simpler and more efficient designs of turboexpanders are possible for heavy-duty vehicles flowrates. Heavy-duty applications of this technology should be explored due to the ease of application and larger potential energy savings.

3. TURBOEXPANDER DESIGN

3.1. Scoping Study

Concurrently with the modeling work performed at SNL, Creare worked on the turboexpander design and efficiency analysis. Before modeling results were obtained from SNL, Creare began a simple trade analysis using fueling data obtained from the NREL dispenser. Initially, assumptions were made to investigate a 50% efficient expander design as a baseline starting point. The results of the scoping study are presented in Table 3.

Table 3. Parameters for Various Expander Designs at 50% Efficiency

Expander Type	Speed	Diameter	Schematic	Radial Load (Est.)	Axial Load (Est.)
Single Radial	195 kRPM	0.63″		0 N*	1 N*
Single Axial	210 kRPM	1.12″		0 N*	>> 100 N
Double Radial	275 kRPM	0.44″		0 N*	0 N*
Double Axial	300 kRPM	0.8″		0 N*	0 N*
Drag	530 kRPM	0.37″		84 N	0 N*

Balancing and loading were explored in the scoping study comparing single and double impeller designs for radial and axial type expanders as well as drag type expanders. With high differential pressures, single impeller designs will have an axial thrust load that will require tight balancing tolerances. Double impeller designs inherently eliminate axial loading by having a symmetrical back-to-back configuration. With each side of the impeller seeing half of the flow, however, the diameter of the impeller is reduced, and the operating speed is much higher. Drag turbines have no axial loading, but since the design is not radially symmetric, a large radial load would be a consideration.

A key finding from the scoping study includes the possibility of using high-speed ball bearings which can be sized appropriately in the 200 kRPM range. Using commercially available ball bearings will present the lowest developmental risk for an initial design compared to hydrodynamic and magnetic bearings. Also explored in the scoping study is the possibility of using commercially available high-speed alternators to couple to the expander. Using standard

14

baseline products will allow for simple trades for evaluating the initial design of a turboexpander.

3.2. Preliminary Expander Design

Creare then began a preliminary expander design based on the scoping study results. Identified operational constraints for this design were defined as a maximum rotational speed of 200,000 RPM and a maximum tip speed of 500 m/s. With these limitations, the maximum efficiency for a single-stage full-admission radial turbine was determined to be 50%. This design has an impeller diameter of 1.26" spinning at 190,000 RPM making a tip speed of 320 m/s. A single-stage radial impeller and design assembly is shown in Figure 11 and Figure 12.
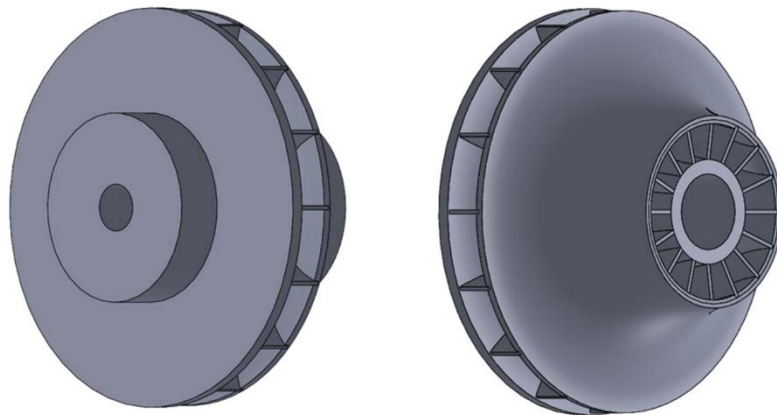

Figure 11. View of Back Side (left) and Front Side (right) of Notional Impeller Design.
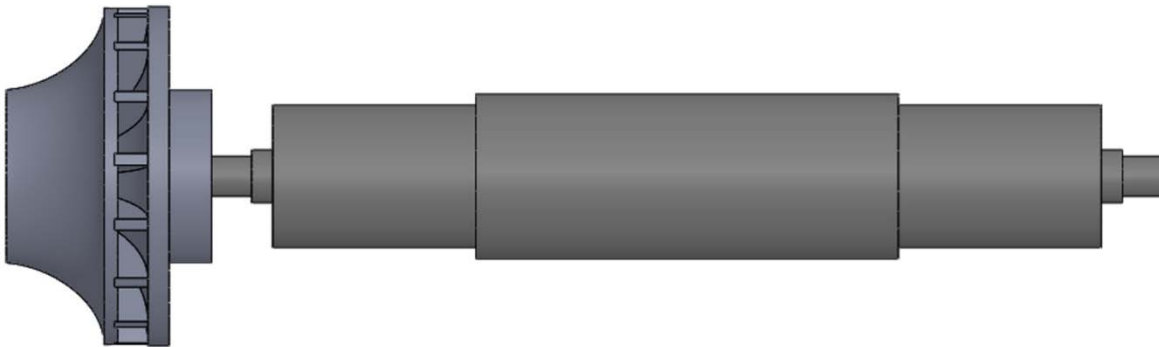
Figure 12. Single-Stage Radial Impeller Design Assembly.

Achieving lower speeds is possible using a partial admission turbine design without increasing tip speed. This single-stage partial admission design would increase the impeller diameter to 4.65" while decreasing the rotational speed to 43,000 RPM. Increasing efficiency using a single-stage partial admission design, however, would quickly exceed the 500 m/s tip speed limitation. As an example, increasing from 50% to 60% efficiency would increase the tip speed form 320m/s to nearly 1,000 m/s. A summary of the single stage designs is shown in Table 4.

Table 4. Parameters for Single-Stage Expander Designs.

Parameter	50% Efficient Full-Admission	50% Efficient Partial-Admission
Diameter	1.26"	4.65"
Rotational Speed	190,000 RPM	43,000 RPM
Tip Speed	320 m/s	320 m/s

The next option considered for increased efficiency is multi-stage expander. Additional stages will increase efficiency while staying within the imposed rotational and tip speed constraints. Multiple stage designs were investigated for partial-admission type expanders with 60%, 70%, and 80% stage efficiency. The overall efficiency increases with the number of stages while staying withing the constraints identified in the scoping study. Efficiencies of up to 88% could be attained using a multi-stage expander design, but the trade-off for this efficiency is increased complexity of the device. A summary of the multi-stage designs is shown in Table 5. A five-stage impeller design is shown in Figures 13 and 14.

Table 5. Parameters for Multi-Stage Expander Designs.

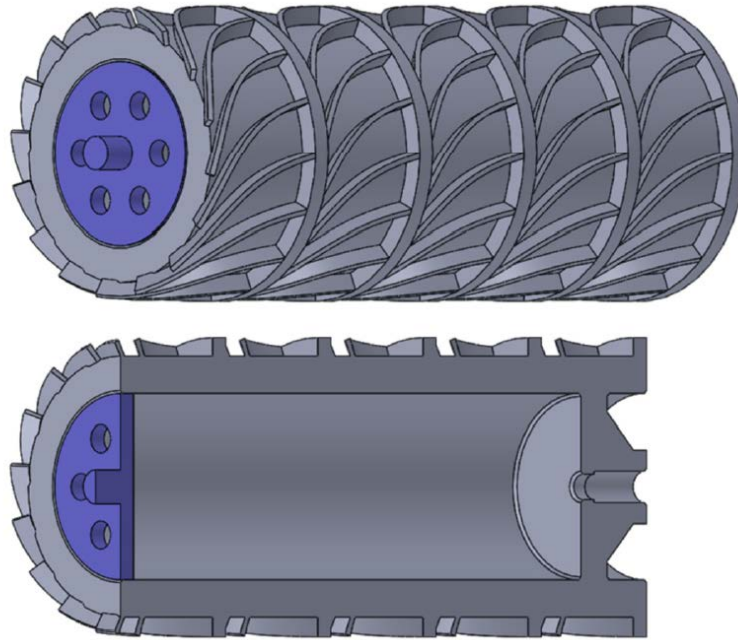| Parameter	60% Stage Efficiency	70% Stage Efficiency	80% Stage Efficiency
Number of Stages	5	7	9
Overall Efficiency	71%	80%	88%
Diameter	1.88"		
Rotational Speed	200,000 RPM		
Tip Speed	500 m/s		

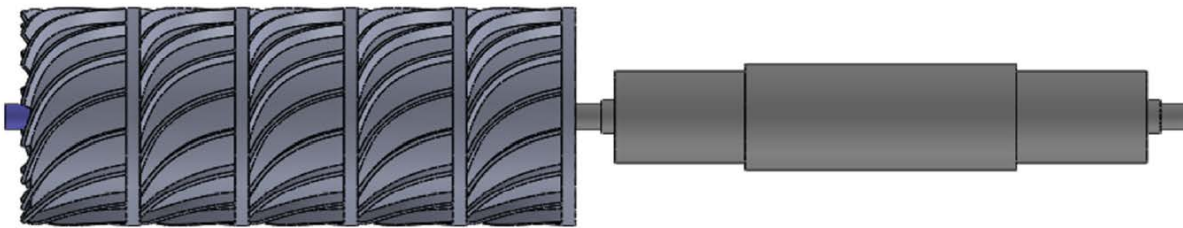**Figure 13. Notional Model of Five-Stage Impeller Design.**

Figure 14. Rotating Assembly with Five-Stage Impeller.

At this point in the design, Creare discussed the path forward with NREL and SNL and a decision was made to continue with a 50% efficient single-stage impeller design for this project. While higher efficiencies would be achievable with multi-stage designs, the SNL modeling had shown a 50% efficient design has the potential to prevent overheating of the vehicle pressure vessel in some cases. It is also beneficial to start with a simpler design as a first step so a baseline can be established with fewer possible failure mechanisms.

3.3. Turboexpander Systems Design

With the impeller sizing, rotational speed, and efficiency requirements decided, Creare began work on designing the rest of the turboexpander systems. The inlet nozzle was the next component that needed to be addressed and a design challenge was immediately apparent. The single-stage full-admission impellor design parameters required extremely small nozzles (<0.001" diameter) and resulted in the need for supersonic flow velocity. To address this issue, Creare proposed a two-expansion stage partial-admission design with the summary of requirements shown in Table 6.

Table 6. Comparison of Single Stage and Two Stage Design with Nozzle Considerations.

Expander Design	Ideal Nozzle Velocity	Impeller Diameter	Operating Speed
Single Stage	Mach > 1.5	1.26"	190,000 RPM
Two Stage	1st Stage: Mach ~1.0 2nd Stage: Mach ~1.0	1.75"	200,000 RPM

While complexity is increased, the updated two-stage design has three main benefits over a single-stage design. First, the nozzle for each stage will be able to stay below sonic flow which will improve efficiency. The need for supersonic flow in a single-stage design would drop the overall efficiency of the turboexpander. Second, the nozzle diameter would be larger allowing for simpler fabrication and improved reliability. Third, the pressure gradient across each stage would be lower which would reduce leakage flow past the impellor.

Each stage in the two-stage design would spin independently and each would act on an independent drive shaft with a layout shown in Figure 15. The flow path would flow from the stage one impellor to the stage two impellor as shown in Figure 16 left. A preliminary partial arc admission impeller design is shown in Figure 16 right.

18
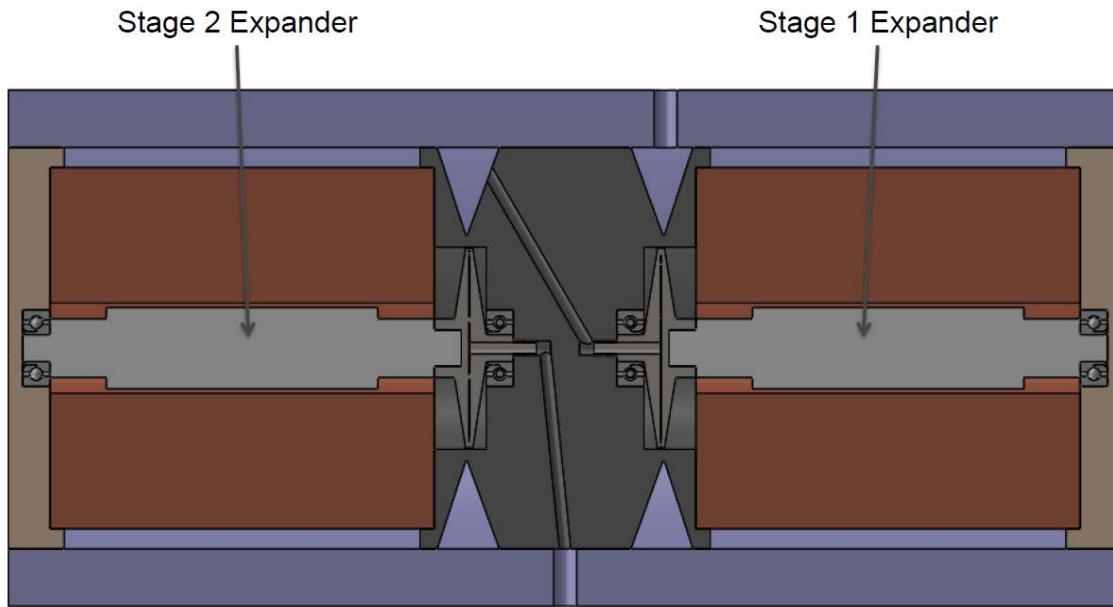
Figure 15. **Two independently rotating stages with equal pressure ratio.**
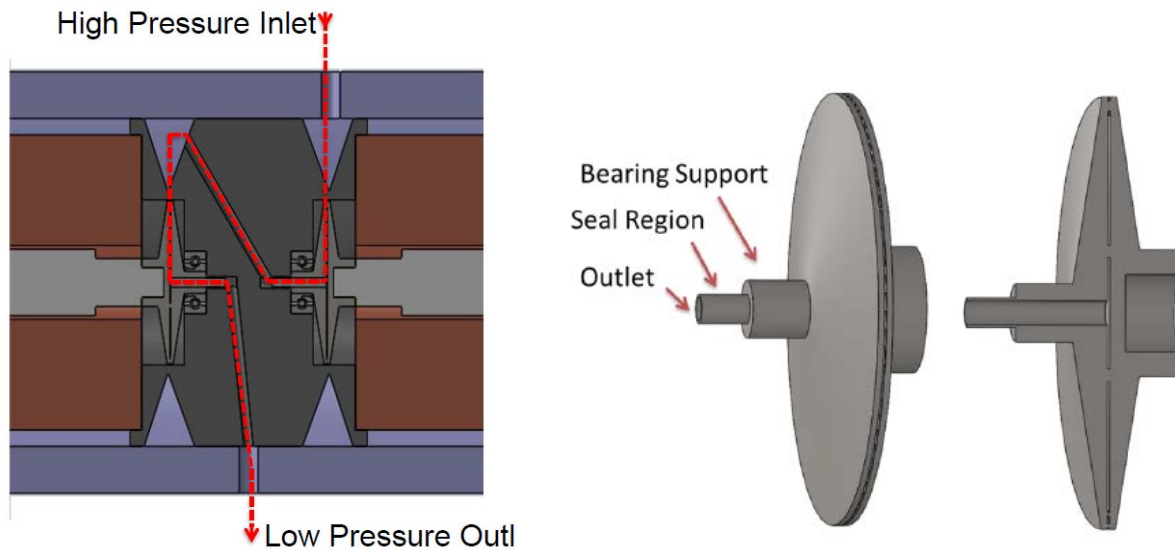
Figure 16. **Two-stage design flow path (left). Preliminary impeller design and cross-sectional view (right).**

3.4.   Integrated System Model

With the advanced layout considerations, Creare created an integrated system model to optimize the performance of the expander. The model includes the effects of leakage flow, flow friction, aerodynamic drag, nozzle velocity, ball bearing friction, and partial admission inefficiency. Overall efficiency for the design is shown to be 52.7% with the two-stage configuration. Results of the model are shown in Table 7.

Table 7. Preliminary Integrated System Model Results

	First Stage	Second Stage	Total
Isentropic Power	27.2 kW	21.2 kW	45.0 kW
Net Shaft Power	12.6 kW	11.1 kW	23.7 kW
Efficiency	46.4%	52.3%	52.7%
Impeller Drag Loss	1.7 kW	0.97 kW	2.67 kW
Alternator Drag Loss	0.65 kW	0.35 kW	1.0 kW
Leakage Flow	1.3%	0.6%	

3.5.   Preliminary Nozzle Design

A preliminary nozzle design shows that the fabrication is feasible with small hole electrical discharge machining (EDM). The first stage would use a partial admission fraction of about 5% (shown in Figure 17) while the second stage would require 10%.
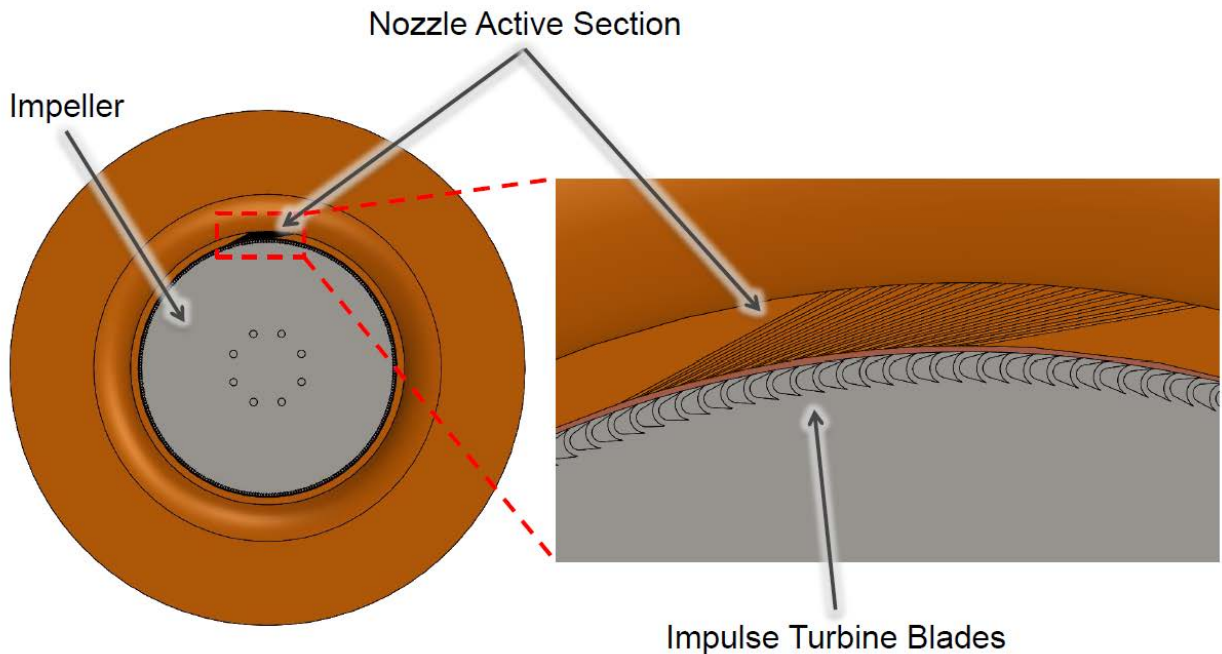
Figure 17. Preliminary Nozzle Design of 1st stage with a partial admission fraction of 5%

3.6.   Turboexpander Design Conclusions

Preliminary design work performed by Creare shows the potential for fabricating a turboexpander that can achieve >50% efficiency. This project only considered pressures and flow rates used in typical light duty hydrogen fueling. Compared to most use cases for turboexpanders, the flow rate in the light duty hydrogen fueling station is quite low. Any

20

potential increase in flow rate would be an overall benefit for the design and efficiency potential of a turboexpander. Heavy-duty hydrogen fueling protocols under development now include higher flow rates. While design work would need to be repeated for heavy-duty fueling specifications, this work suggests that even greater cooling potential exists for the heavy-duty fueling application.

4.   TECHNO-ECONOMIC CASE STUDY

4.1.   Case Study Baseline Conditions

NREL researchers performed a techno-economic case study and compared current cooling needed at a typical station to cooling requirements of a system using a turboexpander. Currently, the SAE J2601 standard requires stations to precool dispensed hydrogen to -40°C before entering the vehicle. The upper boundary of the requirement is -33°C, so most cooling systems are sized according to this boundary. Cooling of the gas can be accomplished in two ways: a large capacity heat exchanger with a moderately sized chiller or a high efficiency heat exchanger with a very large chiller.

The first method is most commonly used by station integrators because conventional off-the-shelf components are available to achieve this cooling. In this method, the heat transfer fluid in the large heat exchanger stores much of the cooling capacity of the cooling system while the chiller cools the fluid as much as possible. The heat transfer fluid in the heat exchanger rises in temperature with every vehicle fill and then the chiller needs time to lower the temperature again. While other environmental factors need to be considered in sizing the heat exchanger, expected vehicle back-to-back fuelings tend to be the most impactful factor in what size heat exchanger is needed. When the heat transfer fluid reaches a temperature that will not allow the dispensed hydrogen to stay below -33°C, the station will be off-line until the chiller can run long enough to bring the temperature back down. Typically, stations are sized to maintain at least 5 back-to-back fills before a cooling down period might be needed. The footprint of the heat exchanger is quite large for the area needed at a dispenser, and so they are often installed in a trench in front of the dispenser. Overhead cooling energy is also a factor that needs to be considered. The chiller will need to run to maintain the heat transfer fluid temperature whether there is a vehicle fueling or not. Temperature loss can be reduced with insulated transfer lines and insulation around the heat exchanger, but with the -33°C requirement, there will always be temperature losses that will incur overhead cooling energy consumption. Figure 18 shows the overhead cooling energy lost when a station is both in use and not used.
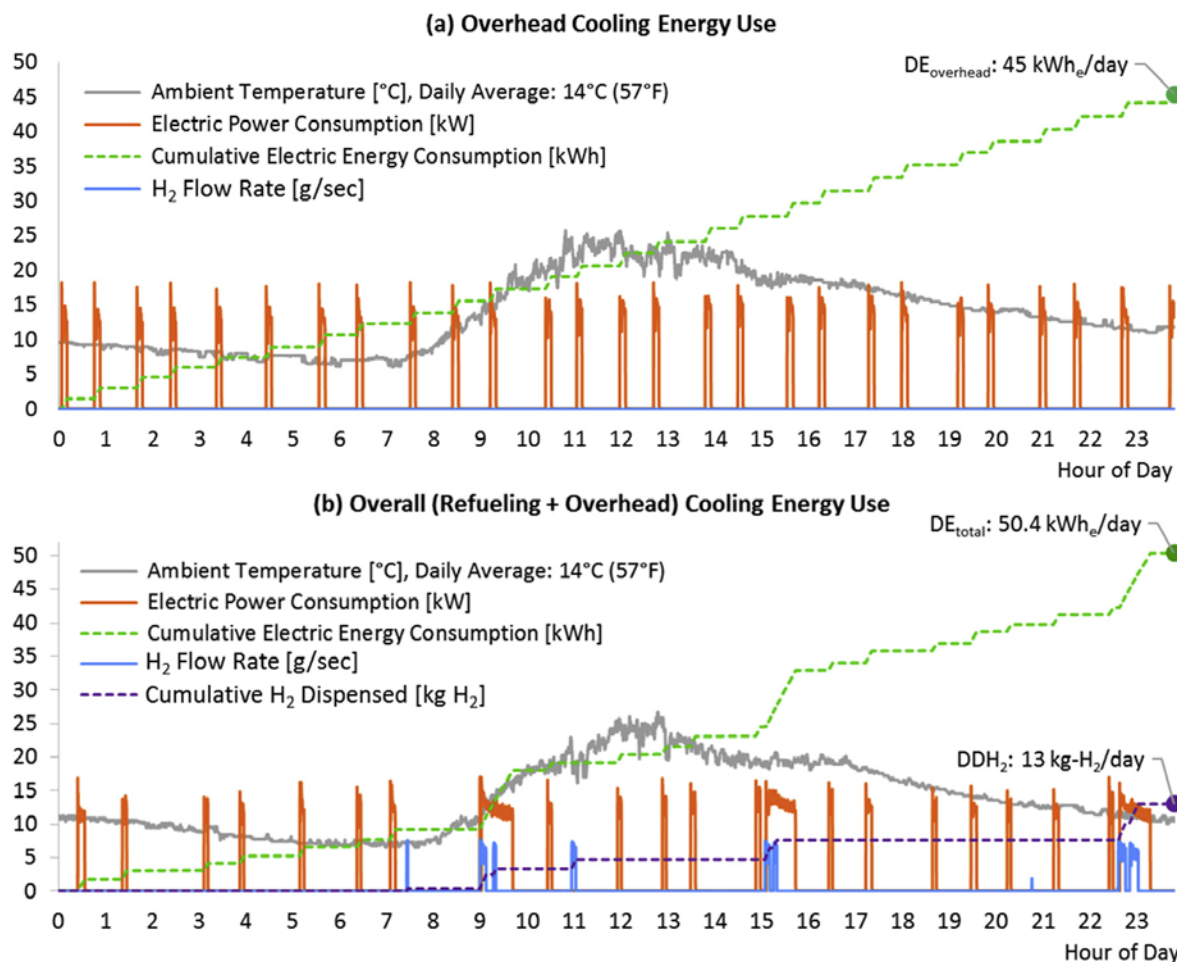
Figure 18. A figure describing overhead cooling energy use at a current station [9].

The second method is not used at any known stations at the time of the case study. In this method, a high efficiency heat exchanger [10] is required that has very little cooling capacity stored in the heat exchanger itself. A drawing of a heat exchanger developed for this purpose can be seen in Figure 19. All the cooling needs to come from the chiller, and so the chiller needs to be very large to accomplish this direct refrigerant cooling. Based on estimates [5], a 37kW cooling capacity chiller is needed to accomplish the cooling needed for this type of heat exchanger. At the time of the case study, the maximum off-the-shelf chiller available was 34kW, so the chiller would need to be a special-order item and may require development. One advantage of this direct refrigerant cooling method is that it can support infinite back-to-back fills because the heat exchanger is not relied upon for any temperature storage capacity. This type of heat exchanger has been demonstrated and has a very small footprint that can fit inside the dispenser cabinet.
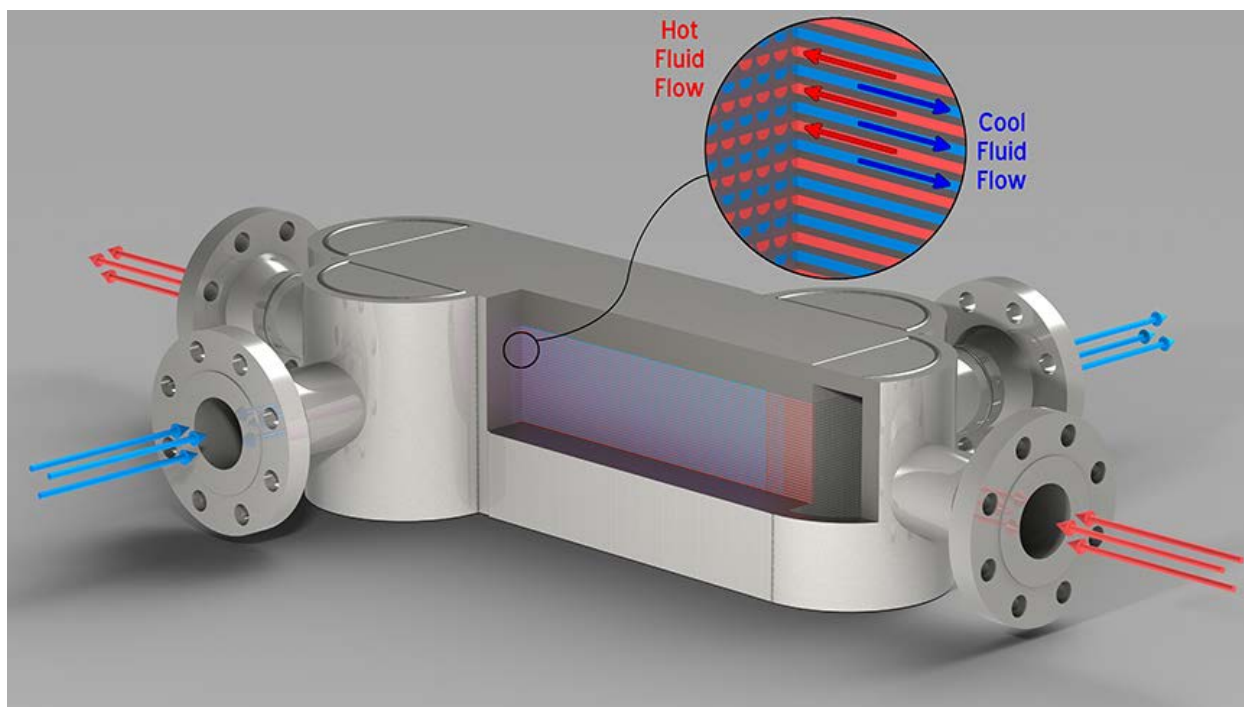
23

Figure 19. A microchannel heat exchanger for hydrogen service. Courtesy of Vacuum Process Engineering, Inc. (VPE) [10].

4.2.   Turboexpander Comparison

Researchers then compared these baseline methods with the potential scenario of a station using a turboexpander for supplemental cooling. With the modeling performed in the project, it was assumed that a chiller and heat exchanger will be needed to maintain 0°C and then the turboexpander would be able to provide the rest of the cooling. In the scenario, the turboexpander was paired with a high efficiency heat exchanger to provide infinite back-to-back fueling capability and small footprint. Like the second method above, the chiller would need to provide all the cooling capacity for the heat exchanger, but the 0°C (-5°C suction temperature) requirement reduces the chiller size quite significantly. Assuming a chiller coefficient of performance of 3, a chiller with an 8kW compressor is needed for this application. This higher temperature requirement along with the smaller chiller size makes the chiller a routine item. The chiller would turn on while hydrogen is being dispensed and will cool directly without the need of a heat transfer fluid storage system. Temperature line loss at 0°C will be minimal with conventional insulation methods and will bring overhead cooling energy use to near zero. The chiller can be placed further away from the dispenser without line losses resulting in easier station design as well as removing any electrical classification requirements for the chiller because it can be placed outside of hazardous area boundaries.

As of 2021, current precooling units that consist of a chiller and large thermal mass heat exchanger have an estimated capital cost of $70,000 [9] for a station with 5 back-to-back fueling capacity. A dispenser that utilizes a turboexpander will be significantly lower in capital expenses. The high efficiency heat exchanger for direct cooling is estimated to cost $12,000 and the 8kW chiller costs $8,500. A turboexpander has not yet been developed, but with industry input is estimated to cost about $15,000 ultimately. Capital cost has the potential to be about half

24

that of current precooling units with the use of a turboexpander. Operational energy use will be reduced by an estimated 45 kWh/day [9] with the reduction of overhead cooling energy use to near zero. Cost savings for this operational consideration will vary by the electrical rate of the station. A comparison summary of conventional vs. this hybrid approach is provided in Table 8.

Table 8. A comparison of a conventional cooling system and a hybrid system.

	Conventional system	Hybrid (turboexpander) system
Heat Exchanger	$55K, 21ft^2	$12K, 1ft^2 (fits inside dispenser)
Chiller	12kW, $130K, 26ft^2	8kW, $8.5K, 9ft^2
Expander	-	$15K, 1ft^2 (fits inside dispenser)
Heat Transfer Fluid	$7K	-
Total Capital Cost	$192K	$35.5K
Total Footprint	47ft^2	9ft^2
Energy Consumption	50 kWh/day	4 kWh/day
Total Operational Cost	$6.5/day	$0.5/day
Back-to-back fills	5	Infinite
Design flexibility of station	Established technology	Robust, compact

4.3.   Case Study Conclusion

Maintenance trade-offs are unknown at this point and are only speculative. The -40°C temperatures have been known to decrease reliability of components [6]. A turboexpander can be placed further down the line in a dispenser so fewer components need to be subjected to low temperature gas. A turboexpander is an additional component that may require a rebuild periodically. Overall, a scenario with a turboexpander installed has the potential to significantly reduce both capital and operating expenses at a hydrogen station. With decreased footprint and capital cost of hydrogen stations, the spread of hydrogen stations may accelerate. As a result of more station and fueling availability, more fuel cell vehicles may be supported by fueling infrastructure.

5.   PROJECT CONCLUSION

NREL, SNL, and Creare worked on a project to model, design, build, and characterize a turboexpander for dispenser precooling. The turboexpander has the potential to provide precooling during fueling events. While the project ended early due to contracting issues, many key findings were made that are worth noting.

Modeling results indicate that a high efficiency turboexpander alone may not achieve enough cooling for light duty dispensing. Putting a turboexpander in line after a smaller chiller and heat exchanger set to 0°C, however, has potential to achieve the needed precooling. A 50% to 60% efficient turboexpander would be able to achieve similar precooling profiles to current requirements when installed this way. Modifications to the fueling protocols would allow for additional pre-cooling in the early stages of the fill to make up for less pre-cooling in the later stages of the fill. Hardware validation is needed to ensure model accuracy and for further model development.

Design results indicate that a >50% efficient turboexpander is achievable for the conditions (pressures and flowrates) found in a light duty hydrogen dispenser. While more development is needed and additional considerations may be needed during a build phase, the initial design was promising. The relatively low flow rate at a light duty dispenser was a key issue identified in the design phase but could be overcome with micro fabrication and multiple stages.

Techno-economic investigation results indicate that the use of a microchannel heat exchanger and a chiller set to 0°C has significant capital and operating cost savings over a typical pre-cooling system at a fueling station. An additional major benefit to this system is the capability to provide unlimited back-to-back fuelings.

While each aspect of this project was geared toward light duty vehicle fueling, many points along the way showed greater potential for a turboexpander using higher flow rates. Heavy duty fueling researchers are currently investigating using higher flow rates with similar pressure profiles. Further design and hardware validation in both areas would be necessary for implementation of a turboexpander precooling system.

6. REFERENCES

[1] *SAE J2601/5 High-Flow Prescriptive Fueling Protocols for Gaseous Hydrogen Powered Medium and Heavy-Duty Vehicles,* SAE International, 2022.

[2] *Fueling Protocols for Light Duty Gaseous Hydrogen Surface Vehicles,* SAE International, 2014.

[3] M. M. Md. Tawhidul Islam Khan, "Characteristics of CFRP Hydrogen Storage Vessel on Rising Temperature in the Filling Process," *Procedia Engineering,* vol. 56, pp. 719-724, 2013.

[4] R. Bozinoski, "MassTran (v0.19.1) Theory Guide," Sandia National Laboratories, Livermore, CA, 2019.

[5] R. Bozinoski and W. S. Winters, "Netflow Theory Manual," Sandia National Laboratories, Livermore, CA, 2016.

[6] T. Bourgeois, T. Brachmann, F. Barth, F. Ammouri, D. Baraldi, D. Melideo, B. Acosta-Iborra, D. Zaepffel, D. Saury and D. Lemonnier, "Optimization of hydrogen vehicle refuelling requirements," *International Journal of Hydrogen Energy,* vol. 42, no. 19, pp. 13789-13809, 2017.

[7] T. Johnson, R. Bozinoski, J. Ye, G. Sartor, J. Zheng and J. Yang, "Thermal model development and validation for rapid filling of high pressure hydrogen tanks," *International Journal of Hydrogen Energy,* vol. 40, no. 31, pp. 9803-9814, 2015.

[8] J. Pratt, D. Terlip, C. Ainscough, J. Kurtz and A. Elgowainy, "H2FIRST Reference Station Design Task: Project Deliverable 2-2," National Renewable Energy Lab, Golden, CO, 2015.

[9] K. R. D.-Y. L. N. R. E. G. Amgad Elgowainy, "Techno-economic and Thermodynamic Analysis of Pre-cooling Systems at Gaseous Hydrogen Refueling Stations," *International Journal of Hydrogen Energy,* vol. 42, p. 29067e29079, 2017.

[10] "DIFFUSION BONDED MICROCHANNEL HEAT EXCHANGERS," Vacuum Process Engineering, Inc. (VPE), [Online]. Available: https://www.vpei.com/diffusion-bonded-microchannel-heat-exchangers/. [Accessed 2022].